

Numerical Analysis of Jets Produced by Intense Laser

Akira Mizuta, Shoichi Yamada, and Hideaki Takabe

*Institute of Laser Engineering, Osaka University, Suita, Osaka, 565-0871, Japan and
Graduate School of Science, Osaka University, Toyonaka, Osaka, 565-0043, Japan*

ABSTRACT

In this paper we present a numerical study of plasma jets produced by intense laser matter interactions. Through this study we hope to better understand astrophysical jets and their recent experimental simulations in the laboratory. We paid special attention to radiation cooling and the interaction of the jet with ambient gas. Four cases are presented in this paper; two of them deal with the propagation of jets in vacuum, while in the other two the propagation takes place in the ambient gas. Available experimental results are reproduced to good accuracy in the vacuum case. For jets in ambient gas, we find that the existence of the surrounding gas confines the jet into a narrow cylindrical shape so that both the density and temperature of the jet remain high enough for effective radiation cooling. As a result, a collimated plasma jet is formed in these cases. The dimensionless parameters characterizing the laboratory jets and protostellar jets have overlapping domains. We also discuss the cooling lengths for our model and compare them with the corresponding values in the astrophysical jets. A plasma jet in the ambient gas experiment is proposed which is within the reach of present day technology, and can be relevant to astrophysical phenomena.

Subject headings: ISM: jets and outflows — hydrodynamics — plasmas — methods: numerical

1. Introduction

Astrophysical jets found in supersonic bipolar flows from black holes, active galactic nuclei (AGN), protostars and similar phenomena are subject to active research. Several problems concerning jets are remaining to be solved, for example, why do the jets propagate such a long distance so stably. Many numerical simulations of astrophysical jets have been performed so far. 2D non-relativistic calculations have been done for AGN jets, by Norman et al. (1982). They found some dimensionless parameters relevant to the propagation of jets

over a long distance. 2D and 3D relativistic calculations have been carried out by Martí et al. (1997); Aloy et al. (1999). Protostellar jets got more attention, detailed numerical simulations have been performed by several authors (see Reipurth, Bally & Devine (1997); Reipurth et al. (1997); Reipurth & Heathcote (1997); Bally & Reipurth (2001) for observational data). Since the radiation cooling and/or external magnetic field are supposed to have very important effect on the plasma jets propagation, radiation hydrodynamic/magnetohydrodynamic codes are essential. For example, Blondin et al. (1990); Stone & Norman (1993) showed with their radiation hydrodynamic codes that the radiation cooling plays an important role for the collimation, leading to the formation of a dense cold shell at the head of the jet. Todo et al. (1993) studied, by means of with MHD code the propagation of jets from young stellar objects into ambient matter, and showed that the azimuthal magnetic field of $\sim 70 \mu\text{G}$ is strong enough to drive a helical kink instability. Since then, many efforts have been put to simulations in 2D and 3D with both radiation cooling and magnetic fields included (Cerqueira & Gouveia Dal Pino 1997; Frank et al. 1998; Gardiner et al. 2000; Frank et al. 2000). The parametric researches that vary the form of the injection, steady or pulsed jets, and the configuration of magnetic field (helical or longitudinal) helped to clarify the systematics of jets. In particular, it was shown that a helical magnetic field can affect the morphology of the head of jets. It was also demonstrated that Kelvin-Helmholtz instability is crucial for the morphology of jets, and linear as well as nonlinear stability analyses were carried out with or without magnetic field to characterize the influence of these factors on the jet shape (Xu et al. 2000; Hardee & Stone 1997; Stone & Hardee 2000; Ryu et al. 2000).

So far these studies are purely theoretical. Recently, however, with the advance of femtosecond laser technology, an experimental investigation of these astrophysical phenomena in the laboratory seems to be possible (Remington et al. 1999, 2000b). This new scientific field is called laboratory astrophysics or laser astrophysics. This progress enable the investigation of radiation hydrodynamics, hydrodynamic instabilities, and similar astrophysical phenomena in model experiments with intense lasers. Such experiments might be able to give us a new and improved insight into those phenomena which could not be obtained by studies of extraterrestrial observations or numerical simulations. Some experiments along these lines have already been carried out, in which hydrodynamic instabilities and the interactions of a strong shock with matter have been measured. Other experiments have been proposed (Remington et al. 2000a). Backup by numerical simulations are indispensable, because they can connect between the processes occurring in laser produced plasmas to astrophysical phenomena that are the aim of our studies. This paper is one of those attempts along this line. In this paper, we will propose a different experiment to understand astrophysical jets.

Some experiments relevant to astrophysical jets have been performed with intense lasers (Farley et al. 1999; Shigemori et al. 2000; Stone & Turner 2000). The so-called 'cone' target

(Fig.1) is employed in those experiments. Another type of experiment has been recently done by Lebedev et al. (2001), using a conical array of fine metric wires. In general, intense laser matter interaction generates high temperature and high density plasma which starts to ablate immediately. If the intensity of laser is $\sim 10^{14} \text{W cm}^{-2}$, the expansion velocity of the plasma reaches a few hundreds of kilometers per second. This is of the same order as the velocity of protostellar jets. This indicates that jets which realistically mimic astrophysical ones can be produced in laboratory. In these experiments, however, the plasma expands into vacuum, and one can not investigate influence of ambient gas, which does exist for the astrophysical jets. As a matter of fact, the ratio of the mass density of the jet to that of the interstellar gas ($\rho_{jet}/\rho_{ambient}$) is $1 \sim 10$ for protostellar jets.

In this paper, we investigate the propagation of laser-produced jets not only in the vacuum but also in the ambient gas using the 2D hydrodynamics code developed recently (Mizuta 2001). Although the code has two versions, relativistic and non-relativistic ones, in the present paper we use only the non-relativistic code.

This paper is organized as follows. In sections 2 and 3, the basic formulas, the numerical method and the initial conditions are presented. The main results are shown in section 4. We discuss some implications to astrophysical jets in section 5 and give a short summary in section 6.

2. Basic Equations and Numerical Method

Assuming a plasma having axial symmetry 2D Euler equation for perfect fluid is solved:

$$\frac{\partial \mathbf{u}}{\partial t} + \frac{1}{r} \frac{\partial(r\mathbf{f})}{\partial r} + \frac{\partial \mathbf{g}}{\partial z} = \mathbf{s}, \quad (1)$$

where the conserved variable vector \mathbf{u} , the flux vectors \mathbf{f} and \mathbf{g} , and the source vector \mathbf{s} are defined as,

$$\mathbf{u} = (\rho, \rho v_r, \rho v_z, E)^T, \quad (2)$$

$$\mathbf{f} = (\rho v_r, \rho v_r^2 + p, \rho v_r v_z, (E + p)v_r)^T, \quad (3)$$

$$\mathbf{g} = (\rho v_z, \rho v_r v_z, \rho v_z^2 + p, (E + p)v_z)^T, \quad (4)$$

$$\mathbf{s} = (0, p/r, 0, 0)^T, \quad (5)$$

$$E = \rho(\epsilon + (v_r^2 + v_z^2)/2). \quad (6)$$

In the above equations, ρ , v_i , p , and ϵ are mass density, i -component of velocity, pressure, and specific internal energy, respectively. We ignore viscosity and heat conduction of the fluid.

These assumptions are justified as follows. As for the collisions, the parameter $\delta = \lambda_{mfp}/L_{sys}$ defined as the ratio of the collisional mean free path λ_{mfp} of electrons or ions and, the characteristic length of the system L_{sys} , is $10^{-4} \sim 10^{-6}$ for our models described below. Hence a hydrodynamic description of the jets is appropriate. Other dimensionless parameters characterizing the dissipative processes are the Reynolds number $Re \equiv r_j v_j / \nu$ which is a measure of the local viscosity and the Peclet number $Pe \equiv r_j v_j / \nu_h$ which describes the heat conduction inside the jet. Here r_j , v_j , ν and ν_h are the radius and velocity of the jet, the viscosity and thermal diffusivity coefficients respectively. Criteria for the influence of these dissipative phenomena on the flow are $Re \lesssim 1$ and $Pe \lesssim 1$. In our models we find $Re \gtrsim 10^9$ and $Pe \gtrsim 10^5$. Thus the neglect of these dissipative processes is well justified. These numbers are evaluated at $t = 2.0$ ns at the center of the inflow region, see below.

An ideal gas equation is used in the computations,

$$p = \rho \epsilon (\gamma - 1), \quad (7)$$

where γ is the adiabatic exponent ($=5/3$ in this paper).

We adopt the Marquina's flux formula (Donat & Marquina 1996) which is based on an approximate Riemann solver derived from the spectral decomposition of the Jacobian matrix of Euler equations. We have developed a computational code which solves Eq. (1) and (7). The code uses cylindrical coordinates with $300(r) \times 1500(z)$ grid points. The accuracy of the code is the second order in space due to a MUSCL method (van Leer 1977, 1979) and is the first order in time.

It is assumed that the plasma is optically thin, so the radiation cooling effect is important. In the cooling term $|J_{rad}|$, only for the bremsstrahlung is included (Zel'dovich & Raizer 1966),

$$|J_{rad}| = 1.42 \cdot 10^{-27} Z^{*2} T^{1/2} n_e n_{ion} \text{erg cm}^{-3} \text{s}^{-1}, \quad (8)$$

where Z^* , T , n_e and n_{ion} are the average ionic charge, temperature and number densities of electron and ion, respectively. The temperature and average ionic charge are related to the specific internal energy ϵ by,

$$\epsilon = \frac{3}{2} \cdot \frac{(Z^* + 1)T}{m_i}, \quad (9)$$

where m_i is the mass of ion. The average ionic charge state Z^* and temperature T were calculated iteratively from local instantaneous density and specific internal energy, as obtained from the hydrodynamic calculation by using Eq.(9) and approximate expression based on the Thomas Fermi model for Z^* (Salzmann 1998). The formulas for the line emission processes

were computed in the usual manner and are not included here for simplicity. As already mentioned the radiation transport is also neglected in this paper. Since we are interested mainly in the qualitative effects of radiation cooling, these approximations are adequate.

We have to distinguish the target matter from the ambient matter in order to make the radiation cooling effective only for the former. For this purpose we introduced another continuity equation for the target matter:

$$\frac{\partial(\rho f)}{\partial t} + \frac{1}{r} \frac{\partial(r \rho v_r f)}{\partial r} + \frac{\partial(\rho v_z f)}{\partial z} = 0, \quad (10)$$

where f is the fraction function. This equation is solved simultaneously with the hydrodynamic equations. With Z^*, T , and f thus obtained, the cooling term is calculated in a separate step. For numerical convenience, the radiation cooling term is turned off for very low temperatures, less than 70 eV. The radiation cooling term is neglected also in the vicinity of the target, where the radiative processes are very complicated and the basic picture of our model is not valid anyway.

3. Initial Condition

In order to simulate the experiments, we put a 'cone' target at an end of the computational region. At $t = 0$, the laser deposits all its energy on the surface. The depth of the surface is $\sim 10\mu\text{m}$. A Gaussian shaped laser pulse of duration of 100ps was assumed. This is much shorter than the dynamical time scale, which is more than a few nanoseconds. When the target made of gold is irradiated by intense laser of $\sim 10^{14}\text{W cm}^{-2}$, the temperature of the target rises to a few hundred eV up to 1 keV, and the ablation takes place. Because the velocity of the ablated plasma is at most its sound velocity, $v_{ab} \sim c_s \sim 10^7\text{cm s}^{-1}$, the ablated plasma expands only up to $\sim 10\mu\text{m}$ during the laser irradiation $\sim 100\text{ps}$. This is much smaller than the scale of the system we consider in this paper. The laser energy deposited into thermal energy is $E_l = 526\text{J}$ for all simulations. Energy of ionization is not included, therefore in a real experiment the incident laser energy, of course, has to be significantly larger.

Four simulations have been done in this paper. In cases 1 and 2, the ambient gas is very dilute ($\rho_a = 10^{-6}\text{g cm}^{-3}$). In the first case, we neglect the radiation cooling, while in the second case the radiation cooling is turned on. These intend to simulate the experiments. In the other two cases, 3 and 4, we let the plasma expansion in the presence of an ambient gas. Case 3 neglects the radiation cooling, and case 4 is done with the radiation cooling term. No corresponding experiments have been carried out as yet. These models serve to clarify the effect of the ambient gas.

The temperature of the target surface, where the laser energy is deposited, increase to ~ 400 eV. The angle of the cone is 126° , which is similar to the experiments (see Fig.2). The target matter is chosen to be gold (^{79}Au) so that we can obtain large effect of the radiation cooling due to a high-Z plasma. The density of the target ρ_t is initially uniform, $\rho_t = 19.2\text{g cm}^{-3}$, and equals to the solid density of the gold. Table 1 summarizes the parameters of the initial conditions.

4. Results

4.1. Vacuum case

First, we discuss cases 1 and 2 which simulate plasma expansion into vacuum. This condition is similar to the experiments of Farley et al. (1999); Shigemori et al. (2000). For numerical reasons, we assumed in these cases as well a cold ($T_a = 0.026\text{eV}$) and very low density ($\rho_a = 10^{-6}\text{g cm}^{-3}$) ambient gas. Due to this very low density this ambient gas had no influence on any of our results. Figure 3 shows the density contours at different times with the radiation cooling off (Fig.3a) and on (Fig.3b), respectively.

In the case of no radiation cooling (Fig.3a), we can see two regions, that is, the inflow region in which matter flows to the axis, and the outflow region. This is schematically shown in Fig.4. Most of the laser-heated matter expands from the target, forming plasma with velocity of a few hundreds of kilometers per second, farther away from the target it converges to the symmetry axis, making a nozzle-like structure in the inflow region. Then, the plasma in the nozzle spouts out from the tip of the nozzle, forming the outflow region. Because the ambient matter is very dilute, there is no pressure support to sustain this nozzle structure. As a result, the outflow spreads out in all directions. This flow structure is suitable for low Z targets, because the effect of the radiation cooling is indeed negligible.

An analysis of the nozzle structure in the inflow region is in order. The converging flow from the cone target to the central axis is very similar with the structure considered by Cantó et al. (1988). From their theoretical model we can estimate the beam radius r_j and velocity v_j from the converging flow angle θ , the reciprocal of the compression ratio ξ between the density of the nozzle to that of the inflow and the velocity of the converging flow v_0 (see Fig.5). These are $\theta = 26.5^\circ$ and $\xi = 1/4$ in our case. Then r_j and v_j are determined as

$$r_j = \frac{\tan \alpha}{\tan \theta + \tan \alpha} y_0, \quad (11)$$

$$v_j = \frac{\cos(\theta + \alpha)}{\cos \alpha} v_0, \quad (12)$$

where y_0 is the width of the inflow and α is the angle between the conical shock and z-axis and given as

$$\tan \alpha = \frac{(1 - \xi) + [(1 - \xi)^2 - 4\xi \tan^2 \theta]^{1/2}}{2 \tan \theta}. \quad (13)$$

Applying this theory to our case with $y_0 = 250\mu\text{m}$ and $v_0 \sim 3 \times 10^7 \text{km s}^{-1}$, we obtain $r_j = 180\mu\text{m}$ and $v_j \sim 1 \times 10^7 \text{km s}^{-1}$, in good agreement with our numerical results.

For high Z targets, we have to consider radiation cooling effects. When radiation cooling is taken into account, the flow structure is changed dramatically (Fig.3b). The plasma in the inflow region is collimated strongly and shows a very thin nozzle at a later time (the radius of the structure is $\sim 40\mu\text{m}$). Although the collimation of the plasma is sustained in the inflow region by converging inflow from the target, the matter again spreads out in the outflow region, resulting in almost the same structure as that for the case without radiation cooling. These experiments are not suitable for the study of the propagation of collimated jets.

Figures 6 a, b and c are the density, pressure and temperature profiles along r -axis, respectively, at $z = 1000\mu\text{m}$, $t = 2.0\text{ns}$. In the case with radiation cooling, the plasma is cooled efficiently around the symmetry axis, leading to the increase of the pressure gradient. As the density increases, the plasma is further cooled, and as a result a jet-like nozzle is formed, which was actually observed in the experiments. Altogether, our simulations support the experimental results that the radiation cooling is a crucial ingredient for the formation of this nozzle.

4.2. Dense gas case

In cases 3 and 4, the ambient matter density was much higher, $\rho_a = 10^{-3} \text{g cm}^{-3}$. The time evolution of hydrodynamics leading to the formation of the inflow and outflow regions is essentially unchanged. Figure 7 shows the density contours at different times with the radiation cooling off (Fig.7a) and on (Fig.7b), respectively. The bow shock, which accelerates the ambient matter, can be seen clearly.

In the case with radiation cooling, the flow structure is dramatically changed as is obvious in Fig.7b. The effect of radiation cooling manifests itself in both the inflow and the outflow regions. In the inflow region, the nozzle structure becomes very thin just like in the vacuum case in the later time. The main difference appears in the outflow region. Unlike all the other cases, the width of the outflow region is very small. Opposed to intuition, this narrow structure is not a direct outcome of the thin nozzle in the inflow region. This is

understood from the second panel of Fig.7b, in which there is already a very thin outflow region while there is no collimated structure in the inflow region. When the matter enters the outflow region, it tends to spread out as in vacuum case. However, the shocked ambient matter slows the expansion in the direction perpendicular to the symmetry axis, and the density and temperature of the flow remain high enough for the radiation cooling to be effective. As a result, a collimated plasma is produced in the outflow region.

This difference of structure in the outer region is remarkable, as is further evident in Fig.8, in which the density, pressure and Mach number profiles along r -axis, respectively, at $z = 2000\mu\text{m}$, $t = 4.0\text{ns}$ are shown. The radius of jet is about $40\mu\text{m}$, and the density ratio is $\eta = \rho_{jet}/\rho_a \sim 100$, namely, this is a so-called dense jet. From Fig.8b, we see that the narrow structure in the outflow region is sustained by the shocked ambient matter, whose pressure is about 1000 times larger than that of the unshocked ambient matter. The jet is supersonic $M_{jet} \sim 70$. The velocity of jet is $\sim 400\text{km s}^{-1}$. This is of the same order as the velocity of protostellar jets. In order to study the propagation of astrophysical jets in the laboratory, we think it is necessary to do experiments with ambient gas.

5. Discussion

Firstly we consider the scaling law between a laboratory jet and a protostellar jet. The velocity of these two jets is almost the same-a few hundred kilometers per second. The ratio of the time scales is, however, widely different 10^{2-4}yr for protostellar jets and 10^{-9}s for laboratory jets, a scale up of a factor of 10^{18-20} . For the experiment to simulate efficiently the astrophysical jet, the ratio of the lengths of jets has to be $\sim 10^{18-20}$. The typical ratio of the radii of the jets (r_{prot}/r_{lab}) is $10^{15}\text{cm}/10^{-3}\text{cm} = 10^{18}$. Thus, the aspect ratios of the jets are close to each other. The temperature is a few eV for both jets, which is consistent with the scaling of velocity mentioned above. Thus, a good scaling law holds between the protstellar jet and the laboratory jet considered in this paper.

The relevant parameters which characterize the jet are the density ratio η , the Mach number and velocity of jets M_{jet} , v_{jet} , the pressure ratio K and the cooling parameter χ . As the magnetic fields were not included our code, no comparison can be made with magnetohydrodynamic simulations (Todo et al. 1993; Cerqueira & Gouveia Dal Pino 1997; Frank et al. 1998; Gardiner et al. 2000; Frank et al. 2000). As is obvious from the results obtained both for the vacuum and the ambient gas cases, the radiation cooling is the most crucial ingredient in the collimation of the jets.

The cooling parameter is defined from the cooling term which has already been employed

in the hydrodynamic simulations, $|J_{rad}|$ in Eq.(8). It is the ratio

$$\chi = \frac{\text{cooling length}}{\text{jet radius}} \sim \frac{v_{jet}\tau_{rad}}{r_{jet}}, \quad (14)$$

where v_{jet} and r_{jet} are the velocity and radius of jet, respectively, and τ_{rad} is a characteristic radiation cooling time. τ_{rad} is defined from the ratio of thermal energy density to emission power as

$$\tau_{rad} = \frac{e_{thr}}{|J_{rad}|}. \quad (15)$$

The smaller χ is, the more effective the cooling is. The cooling term adopted in Eq.(8) is different from those used in other papers (Blondin et al. 1990; Stone & Norman 1993). We assumed in this paper that the jet matter is Au, rather than hydrogen in most other papers. Our choice was influenced by the need to enhance the radiation cooling so that the hydrodynamics is affected within a few nanoseconds. In fact, the average ionic charge state Z^* is about 20 – 40 for $T = 50 - 100\text{eV}$. Although the detailed dependence on T is different between our cooling term and others, it is emphasized that the dynamics should be similar as long as the cooling parameter χ has a similar value during the greater part of the time evolution.

In case 4 (with dense ambient gas and radiation cooling), the typical radiation cooling time is $\tau_{rad} \sim 10\text{ns}$ at $t = 1.0\text{ns}$, and $\tau_{rad} \sim 100\text{ns}$ for $t = 4.0\text{ns}$. These were evaluated at the points with the largest emission power. Accordingly, the radiation cooling parameters for each time are $\chi \sim 10$ and $\chi \sim 100$, respectively. Thus, the radiation cooling is effective for the earlier phase, while the jet is cool enough, while the radiation cooling is ineffective for the later phase. However, it is noted that we underestimate the radiation cooling, since we neglected the line emissions which could be substantial in our cases, and take into account only the bremsstrahlung. This was done mainly to keep numerical simplicity.

The aim of our calculations and future experiments is to understand better the physics of protostellar jets. Although the observational values of physical quantities are rather uncertain, they are typically, $n_e \sim 10^3\text{cm}^{-3}$, $T_j \sim 10^4\text{K}$, $v_j \sim 100\text{km s}^{-1}$ and $r_j = 10^{15}\text{cm}$ (Bally & Reipurth 2001). These values roughly correspond to $\eta \approx 1 - 10^3$, $M_{jet} \approx 1$ with the main uncertainty coming from the lack of data on the density and temperature of the ambient matter. From these parameters, it is estimated that the total emission power is $|J_{rad}| \sim 10^{-18}\text{erg cm}^{-3}\text{s}^{-1}$ for collisional by excited hydrogen atoms (Dalgarno & McRay 1972). The emission power due to the bremsstrahlung is $|J_{rad}| \sim 10^{-19}\text{erg cm}^{-3}\text{s}^{-1}$. Thus the bremsstrahlung is substantially weaker, and in general the bound-bound emission is dominant in such plasmas. The emission power $|J_{rad}| \sim 10^{-18}\text{erg cm}^{-3}\text{s}^{-1}$ gives a cooling time of $\tau_{rad} \sim 10^9\text{s}$, which then leads to a cooling parameter of $\chi \sim 10$. It is evident from

these values that the experimental values used in this paper are appropriate for studying astrophysical jets. As mentioned in the introduction, Blondin et al. (1990); Stone & Norman (1993) studied the properties of propagating jets by varying η between 1 and 10. Their parameters correspond to χ between 0.1 and 10. We think that our results have overlapping region to the initial conditions of those papers. This means that the experiments proposed here might give some new insights into the astrophysical jets studied theoretically in their papers.

6. Conclusion

In this paper results of four hydrodynamic simulations have been shown, in which jet were generated from 'cone' target irradiated by intense laser. In all the simulations, we have found a common feature, that is, the existence of an inflow region and an outflow region. Depending on whether the radiation cooling is turned on or off, and whether there is some ambient gas or not, the flow structure inside these regions is very different from each other.

When the plasma flows into a very low density ambient gas, the collimation of the plasma jet occurs only due to radiation cooling. With radiation cooling, the collimated plasma shows up in the inflow region. However, since the structure is sustained by converging inflow from the target, it disappears in the outflow region, in which there is no pressure support to maintain it. This feature is very similar to that found in the experiments. We have also found that the nozzle structure with no radiation cooling is well described with the analytical model by Cantó et al. (1988)

In the case with ambient gas, a bow shock appears very clearly. The main difference between the vacuum and dense gas cases is that in the latter case the collimated flow appears not only in the inflow region but also in the outflow region. Particularly, the collimated plasma in the outflow region is sustained by the pressure of the shocked ambient matter.

We have shown the possibility to carry out a laboratory experiment, using high intensity laser-plasma interaction, to generate collimated plasma jets propagating into an ambient gas. The parameters of such plasma jet are similar to those of protostellar jets. If such an experiment is performed, we can get important information about the physics of astrophysical jets.

External magnetic fields were not included in our calculations. Experiments with magnetic fields have already proposed and will be carried out in the future. We intend to adjust our simulations to the needs of future experiments.

This work was carried out on NEC SX4, Cybermedia Center Osaka Univ. and HITACHI SR8000, Institute of Laser Engineering, Osaka Univ.

One of authors (A. Mizuta) would like to thank K. Sawada, H. Nagatomo and N. Ohnishi for good suggestions for numerical methods.

REFERENCES

- Aloy, M. A., Ibáñez, J. M^a., Martí, J. M^a., Gómez J. L., & Müller, E., 1999, ApJ, 523, L125
- Bally, J. & Reipurth, B., 2001, ApJ, 546, 299
- Blondin, J. M., Fryxell, B. A., & Königl, A., 1990, ApJ, 360, 370
- Cantó, J., Tenorino-Tagle, G., & Różyczka 1988, A&A, 192, 287
- Cerqueira, A. H., & de Gouveia Dal Pino, E. M., 1997, ApJ, 489, L185
- Dalgarno, A. & McRay, R. A., 1972, ARA&A, 10, 375
- Donat, R., & Marquina, A., 1996, J. Comput. Phys., 125, 42
- Farley, D. R. et al. 1999, Phys. Rev. Let., 83, 1982
- Frank, A., Lery, T., Gardiner, T. A., Jones, T. W., & Ryu, D., 2000, ApJ, 540, 342
- Frank, A., Ryu, D., Jones, T. W., & Noriega-Crespo A., 1998, ApJ, 494, L79
- Gardiner, T. A., Frank, A., Jones, T. W., & Ryu, D., 2000, ApJ, 530, 834
- Hardee, P. E., & Stone, J. M. 1997, ApJ, 483, 121
- Lebedev, et al. 2001, ApJL, submitted (astro-ph 0108067)
- Martí, J. M^a., Müller, E., Font, J. A., Ibáñez, J. M^a., & Marquina, A., 1997, ApJ, 479, 151
- Mizuta, A., 2001, Master thesis Osaka Univ.
- Norman, M. L., Smarr, L., Winkler, K.-H., & Smith, M. D., 1982, A&A, 113, 285
- Reipurth, B., Bally, J., & Devine, D., 1997, AJ, 114, 2708.
- Reipurth, B., Hartigan, P., Heathcote, S., Morse, J. A. & Bally, J., 1997, AJ, 114, 757.

- Reipurth, B. & Heathcote, S., 1997, in Herbig-Halo Flows and the Birth of Low Mass Stars, in IAU Symposium no.182, eds Reipurth, B. & Bertout, C., 3.
- Remington, B. A., Arnett, D., Drake, R. P., & Takabe, H., 1999, Science, 284, 1488
- Remington, B. A., Drake, R. P., Arnett, D., & Takabe, H. (Editors), 2000, ApJS, 127, No.2, Part1
- Remington, B. A., Drake, R. P., Takabe, H., & Arnett, D., 2000, Phys. Plasmas, 7, 1641
- Ryu, D., Jones, T. W., & Frank, A. 2000, ApJ, 545, 475
- Salzmann, D., 1998, Atomic Physics in Hot Plasmas, (New York:Oxford University Press)
- Shigemori, K. et al., 2000, Phys. Rev. E, 62, 8838
- Stone, J. M., & Hardee, P. E. 2000, ApJ, 540, 192
- Stone, J. M., & Norman, M. L., 1993, ApJ, 413, 198
- Stone, J. M., Turner, N., Estabrook, K., Remington, B., Farley, D., Glendinning, S. G., & Glenzer S., 2000, ApJS, 127, 497
- Todo, Y., Uchida, Y., Sato, T., & Rosner, R., 1993, ApJ, 403, 164
- van Leer, B., 1977, J. Comput. Phys., 23, 276
- van Leer, B., 1979, J. Comput. Phys., 32, 101
- Xu, J., Hardee, P. E., & Stone, J. M., 2000, ApJ, 543, 161
- Zel'dovich, Ya. B. and Raizer, Yu. P., 1966, Physics of Shock Waves and High-Temperature Hydrodynamic Phenomena, vol. I, (New York:Academic Press)

Table 1: Detailed parameters for initial condition. ρ and T mean density and temperature. Index 't' and 'a' stand for target and ambient matter

	case1	case2	case3	case4
target	Au			
$\rho_t \text{g cm}^{-3}$	19.2			
$T_t \text{eV}(\text{hot/cold})$	676/1.77			
$\rho_a \text{g cm}^{-3}$	10^{-6}		10^{-3}	
$T_a [\text{eV}]$	0.026			
cooling term	OFF	ON	OFF	ON

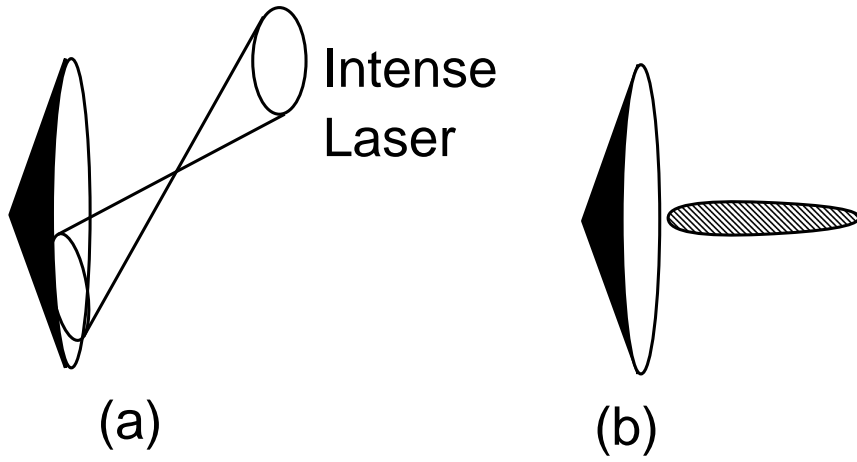


Fig. 1.— 'Cone' target. (a):Some intense lasers irradiate on the 'cone' target surface. (b):Ablation plasma will collimate and become a jet-like structure.

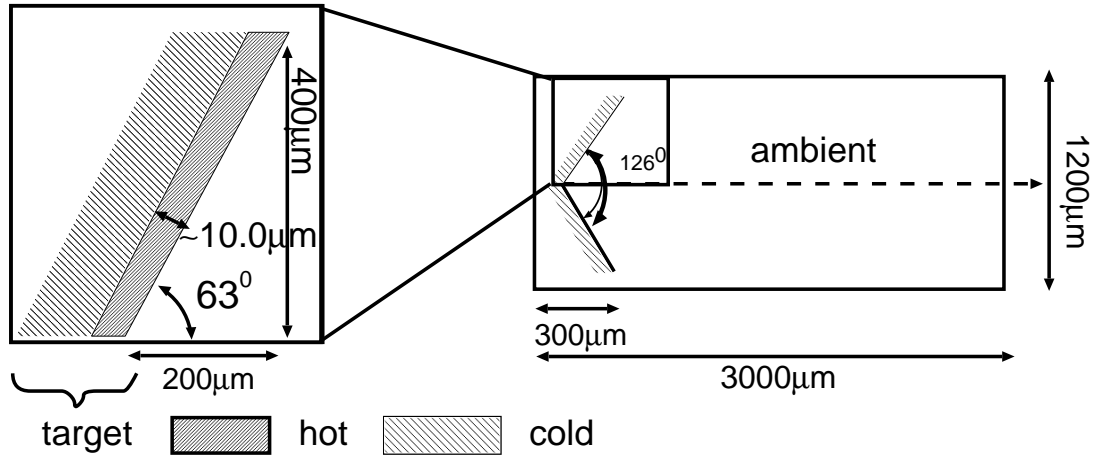


Fig. 2.— Initial conditions. The cone target is set at the left end of computational region ($1200\mu\text{m} \times 3000\mu\text{m}$). Hot plasma is put at the surface. It's depth is $\sim 10\mu\text{m}$.

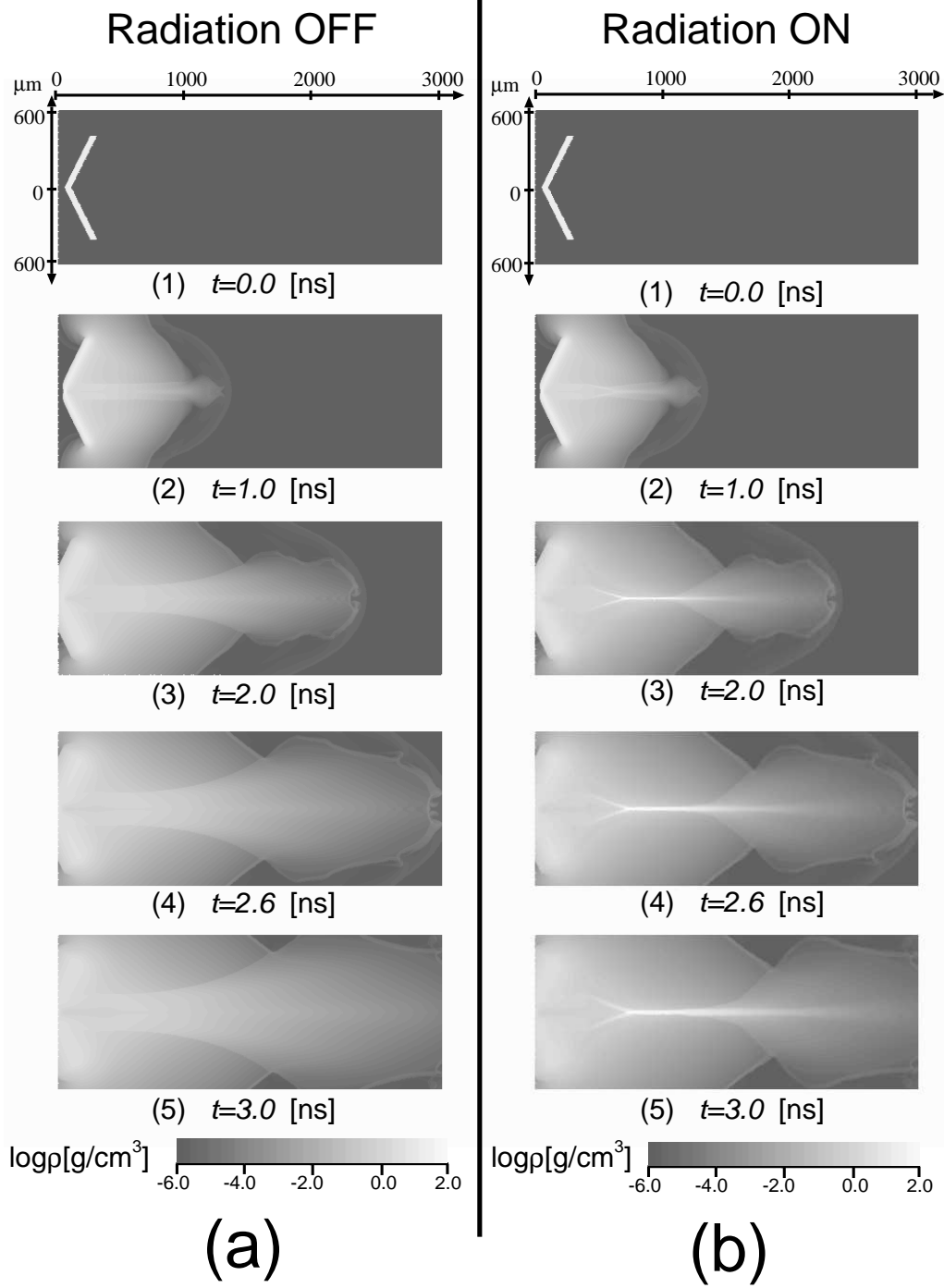


Fig. 3.— Density profiles in $r - z$ plane, in the vacuum case; (a) radiation off(case1), (b) radiation on(case2). $t = 0.0(1), 1.0(2), 2.0(3), 2.6(4), 3.0(5)$ ns

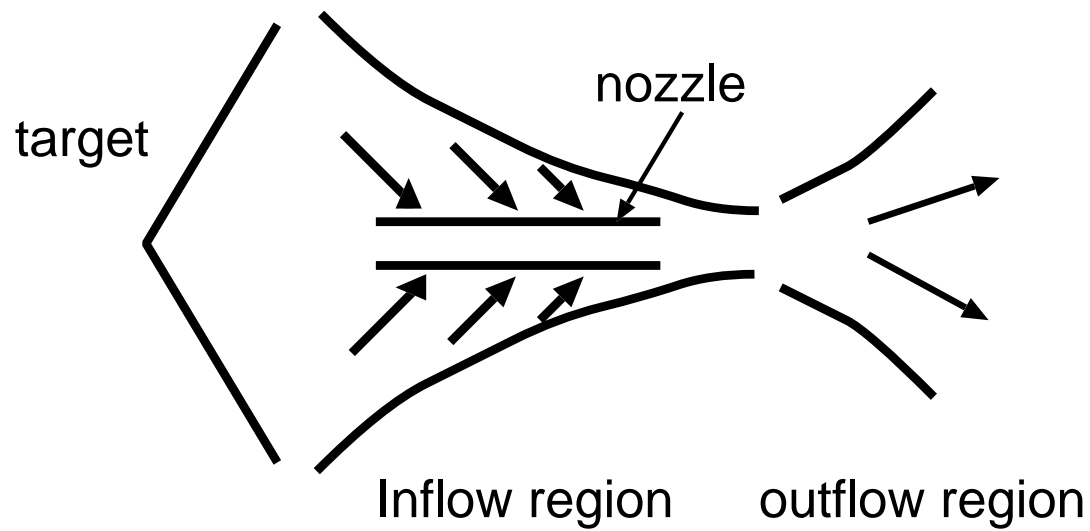


Fig. 4.— Schematic flow structure. The flow is divided to two regions, inflow and outflow region.

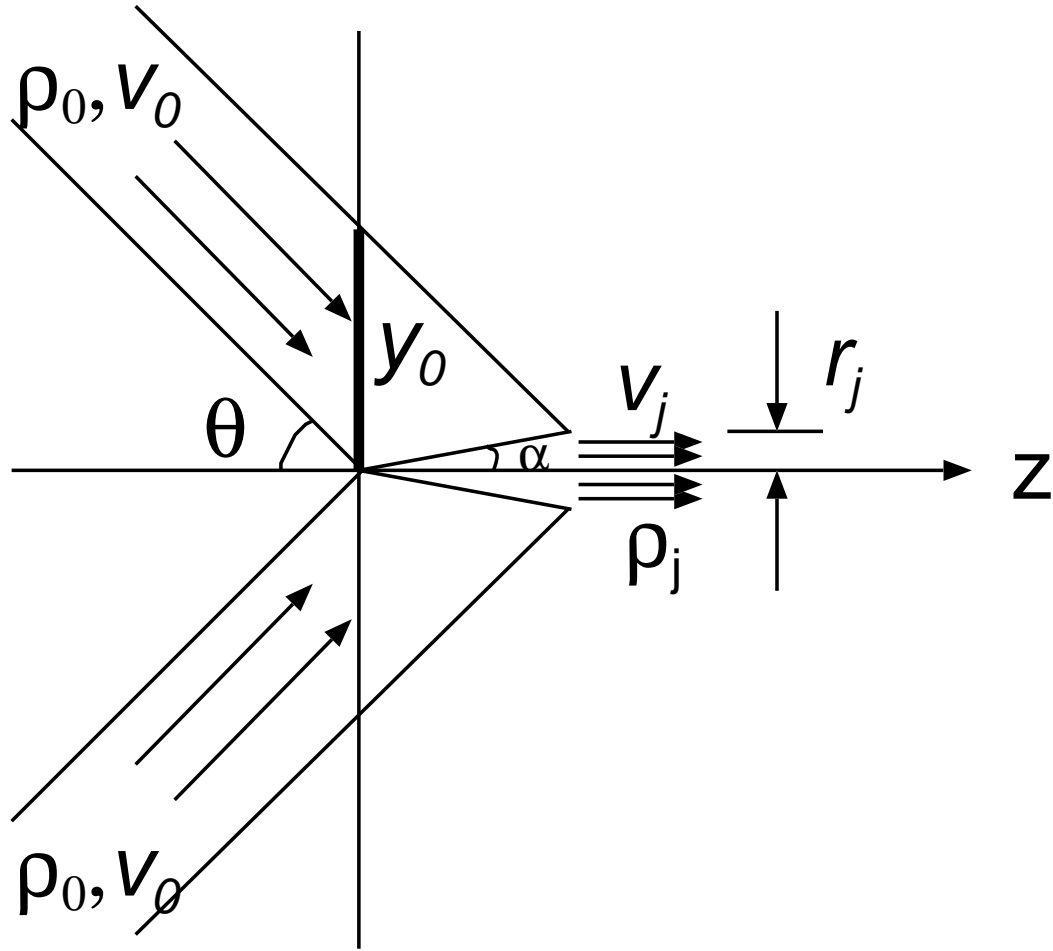


Fig. 5.— A schematic drawing of the conical flow to the central axis.

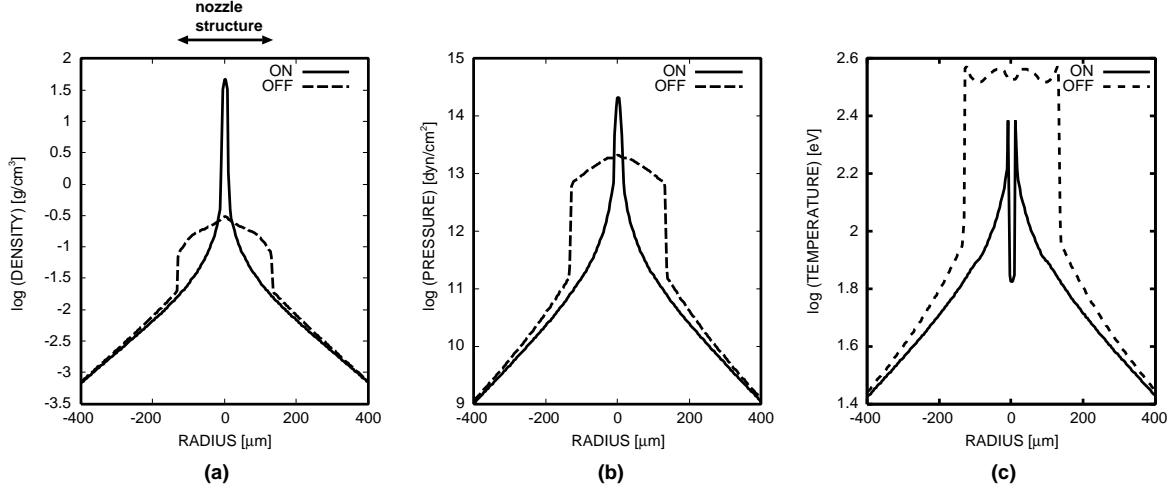


Fig. 6.— Density, pressure and temperature profiles along r axis at $z=1000\mu\text{m}$, $t=2.0\text{ns}$. The radiation cooling term is OFF(dash line,case 1) and ON(solid line,case 2).

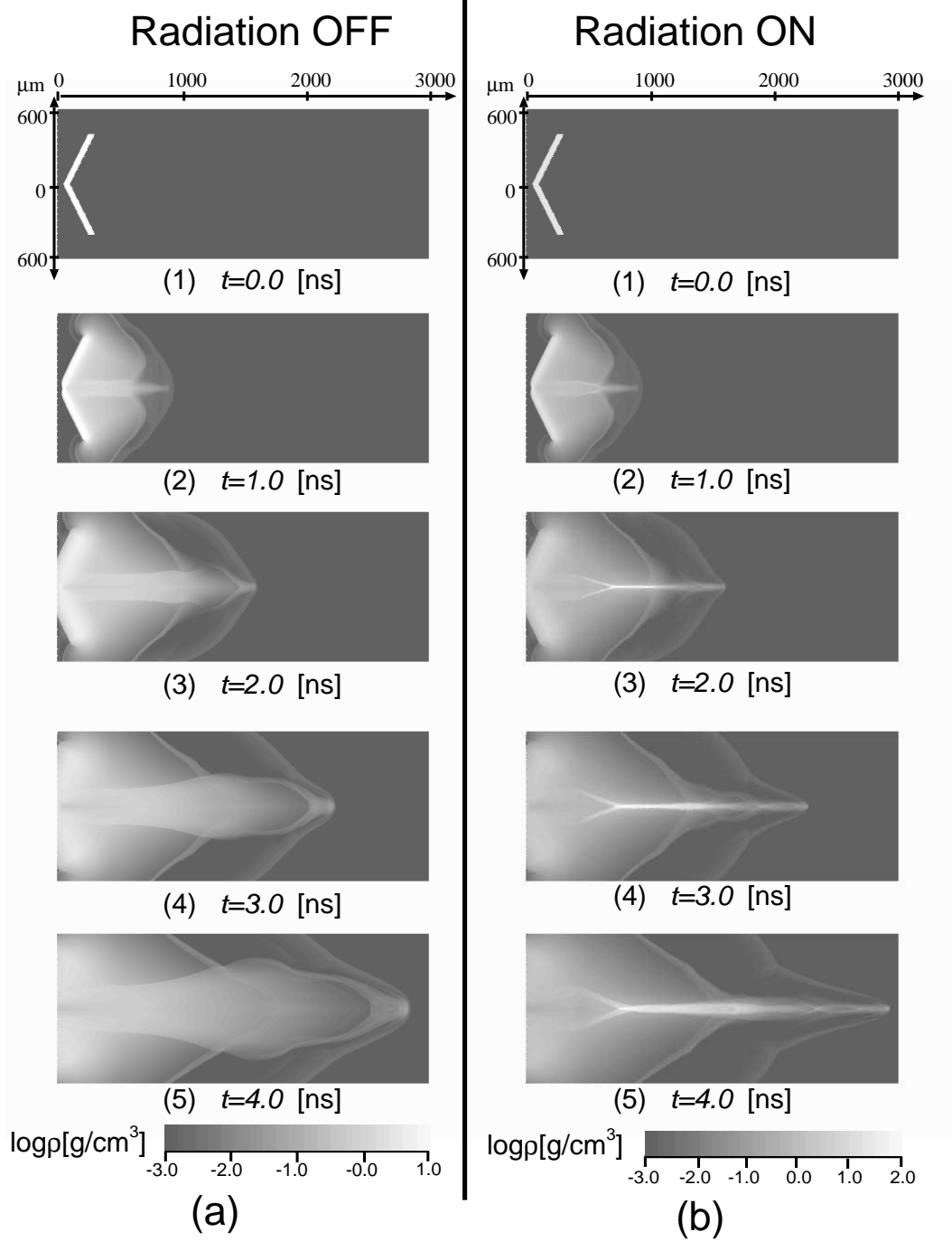


Fig. 7.— Density profiles in $r-z$ plane, in the dense gas case; (a) radiation off(case3), (b) radiation on(case4). $t = 0.0(1), 1.0(2), 2.0(3), 3.0(4), 4.0(5)$ ns

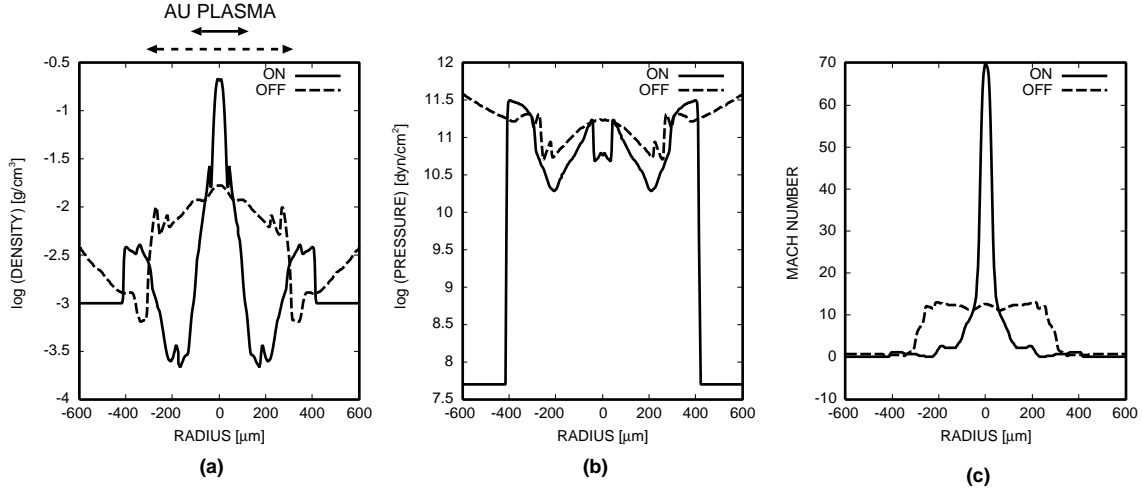


Fig. 8.— Density, pressure and Mach number profiles along r axis at $z=2000 \mu\text{m}$, $t=4.0 \text{ ns}$. The radiation cooling term is OFF(dash line,case 3) and ON(solid line,case 4).